JOURNAL OF ADVANCED DIELECTRICS
Vol. 9, No. 5 (2019) 1950039 (7 pages)

DOI: 10.1142/S2010135X19500395

World Scientific
www.worldscientific.com

Raman wavenumbers calculated as a function of pressure from the mode Grüneisen parameter of PZT ($x = 0.48$) ceramic close to the monoclinic-cubic transition

A. Kiraci
Inter-Curricular Courses Department
Cankaya University, Ankara, Turkey
akiraci@cankaya.edu.tr

Received 14 June 2019; Accepted 7 October 2019; Published 5 November 2019

The isothermal mode Grüneisen parameter $\gamma_T(P)$ of some Raman modes in $PbZr_{1-x}Ti_xO_3$ (PZT, $x = 0.48$) were calculated as a function of pressure by means of the observed pressure-dependent volume data of PZT ($x = 0.48$) crystal from the literature at room temperature of 298 K. Those calculated values of $\gamma_T(P)$ were then used to compute the pressure dependence of the Raman modes in PZT ($x = 0.48$) ceramic studied here. The observed and calculated values of the Raman wavenumbers in PZT were in good agreement, which indicates that the isothermal mode Grüneisen parameter can also be used to predict the pressure-dependent wavenumbers of some other perovskite-type crystals. Additionally, the pressure dependence of the thermodynamic quantities such as isothermal compressibility κ_T, thermal expansion α_P and the specific heat $C_P - C_V$ of PZT ($x = 0.48$) ceramic were predicted at constant temperature of 298 K. Here, the experimentally measurable thermodynamic quantities calculated for PZT ($x = 0.48$) ceramics provide theoretically a significant opportunity for testing.

Keywords: Grüneisen parameter; Raman wavenumbers; PZT ($x = 0.48$); specific heat; thermal expansion.

1. Introduction

Inorganic $PbZr_{1-x}Ti_xO_3$ (PZT) ceramics are widely used in electronic devices as ultrasound generators and micro positioners due to their important piezoelectric, dielectric and ferroelectric properties that depend strongly on their structural phase. The phase transition mechanism of PZT ceramics are very complicated depending on the various compositions (value of x). It is reported that PZT ceramics have cubic perovskite structure at high temperatures with a space group $Pm\bar{3}m - O_h^1$ and they undergo a phase transition at about 667 K[1–3] (or 650 K[4,5]) to rhombohedral phase with a space group $R3m - C_{3v}^5$ for Zi rich samples ($x < 0.5$) and to tetragonal phase with a space group $P4\,mm - C_{4v}^1$ for Ti rich samples ($x > 0.5$). In their high synchrotron X-ray experiments at low temperatures, Noheda *et al.*[6,8] noticed the existence of a third phase (first monoclinic phase) with a space group $Cm - C_s^3$ that is the separation between tetragonal and rhombohedral phases, namely the morphotropic phase boundary (MPB) for values of x close to 0.48.[4] It is also reported that close to the room temperatures for $x = 0.48$ in PZT ceramics, the monoclinic phase transforms to the tetragonal phase.[8] Ragini *et al.* have reported a second monoclinic phase with a space group $Cc - C_s^4$ below 210 K for $x = 0.48$ via an antiferrodistortive phase transition.[9–11] It is noted that diversity of the sample fabrication methods and the grain sizes make it difficult to define the existence and nature of the monoclinic phase in PZT ceramics near MPB.[12,13] The highest piezoelectric response of PZT ceramics were reported to be the compositions near the MPB around $x = 0.45 - 0.50$.[14]

Various experimental techniques have been applied to understand the structure and phase transition mechanism of PZT ceramics near the MPB, including infrared spectroscopy,[15–17] dielectric measurement,[9] Raman spectroscopy,[18–21] X-ray powder diffraction,[22] time-domain terahertz and microwave spectroscopy.[23] The dielectric and piezoelectric properties of PZT ceramics have been investigated by applying external or electric fields.[24–28] The P-T phase diagram of PZT ($x = 0.48$) ceramic has also been reported in the literature.[20,29] Also, a theoretical electromechanical study has been reported for PZT ceramic close to the MPB.[30] Recently, we have calculated the damping constant (linewidth) and the relaxation time of the Brillouin LA mode as a function of temperature close to the ferroelectric−paraelectric phase transition in PZT ($x = 0.45$).[31]

Group theory analysis predicted[32] seven simultaneous Raman and infrared (IR) active plus one Raman active modes $[3A_1(IR,R) + 4E(IR,R) + 1B_1(R)]$ in the tetragonal ($P4\,mm$ group) phase for a perfectly oriented single PZT crystal, while seven Raman and IR active modes $[3A_1(IR,R)+4E(IR,R)]$ have been predicted in the rhombohedral ($R3m$ group) phase of PZT. It has also been reported[33] that, on lowering the temperature, the rhombohedral phase transforms into the $R3c$

space group with 13 Raman and IR optic modes [$4A_1$(IR,R)+ 9E(IR,R)] and the tetragonal phase transforms into the I4 cm group with 13 simultaneous Raman and IR plus 3 Raman optic modes [$4A_1$(IR,R)+8E(IR,R)+$1B_1$(R)+$2B_2$(R)]. On the contrary to the prediction from the group theory, much more Raman modes are observed for PZT near the MPB due to the strong splitting between the longitudinal optic (LO) and transverse optic (TO) modes.[34]

As a dimensionless quantity, Grüneisen parameter describes the thermoelastic behavior of materials at high pressures and temperatures. It is not only defined microscopically but also macroscopically. Microscopic definition (γ_i) relates Grüneisen parameter to the vibrational wavenumbers of the lattice modes, while macroscopic definition (γ) relates it to the familiar thermodynamic quantities such as thermal expansion, isothermal compressibility and heat capacity. It is pointed out that the sum of all γ_i throughout the first Brillouin zone leads to a macroscopic definition of Grüneisen parameter γ[35] The Grüneisen parameter in the case of the bridge allows the calculation of the macroscopic thermodynamic quantities in terms of the microscopic quantity such as wavenumbers shifts of crystals. Although it is very difficult to determine γ experimentally due to the requirement of a detailed knowledge of the phonon dispersion spectrum of a material and/or experimental measurements of thermodynamic properties at high pressures and temperatures, a number of approximate expressions have been suggested[36] to get an accurate value for it.

By following our recent work,[37] in this study the isothermal Grüneisen parameters of the observed[20] Raman modes in PZT ceramic ($x = 0.48$) were determined by using the V-P relation[38] of this ceramic at room temperature close to the monoclinic-cubic phase transition pressure of $P_C = 5$ GPa. This V-P relation[38] for PZT ceramic ($x = 0.48$) was also used to predict the isothermal compressibility κ_T of this ceramic as a function of pressure up to the 17 GPa at $T = 298$ K. By using the definition of the isothermal Grüneisen parameter $\gamma_T(P)$, the pressure dependences of the Raman shifts for the observed modes[20] in PZT ceramic studied have been calculated. Also, the thermal expansion α_P and the specific heat $C_P - C_V$ of PZT ($x = 0.48$) ceramic were predicted as a function of pressure by using the observed[20] P-T phase diagram of this crystal close to the monoclinic-cubic transition.

In Sec. 2, the "calculations and results" are given. The "discussion" and "conclusions" are given in Secs. 3 and 4, respectively.

2. Calculations and Results

The Grüneisen parameter γ, that measures the unharmonicity of a crystalline system, is defined microscopically in terms of the volume (V) dependence of the vibrational wavenumbers (f) of the lattice modes as

$$\gamma = -\frac{\partial \ln f}{\partial \ln V}, \tag{2.1}$$

from Eq. (2.1), the isothermal Grüneisen parameter $\gamma_T(P)$ can be written as

$$\gamma_T(P) = -\frac{V(P)}{f(P)} \frac{(\partial f/\partial P)_T}{(\partial V/\partial P)_T}, \tag{2.2}$$

integrating Eq. (2.2), one gets the pressure dependence of the wavenumbers $f_T(P)$ at constant temperature as

$$f_T(P) = A(P) + f_1 \exp\left[-\gamma_T \ln\left(\frac{V_T(P)}{V_1}\right)\right]. \tag{2.3}$$

Here, f_1 and V_1 are the wavenumbers and the volume of the vibrational modes at ambient conditions ($T = 298$ K, $P = 0$), respectively while P is the pressure. The pressure-dependent $A(P)$ term in Eq. (2.3) is a second-order correction function that can be evaluated through a fitting procedure, given as

$$A(P) = a_0 + a_1 P + a_2 P^2, \tag{2.4}$$

where a_0, a_1 and a_2 are constants with appropriate units.

The isothermal Grüneisen parameter of the Raman modes in PZT ($x = 0.48$) ceramic was calculated here according to Eq. (2.2). For this calculation, the observed[20] Raman shifts data and the observed[38] volume data were analyzed as a function of pressure as

$$f = b_0 + b_1 P + b_2 P^2, \tag{2.5}$$

and

$$V = c_0 + c_1 P + c_2 P^2, \tag{2.6}$$

the fitting parameters b_0, b_1, b_2 of Eq. (2.5) and c_0, c_1, c_2 of Eq. (2.6) were given in Tables 1 and 2, respectively in the pressure intervals indicated. The calculated values of $\gamma_T(P)$ for the Raman modes in PZT ceramic studied here were given in Figs. 1 and 2 as a function of pressure. Once the isothermal Grüneisen parameter $\gamma_T(P)$ by using Eqs. (2.5) and (2.6) it was easy to calculated the wavenumbers of the Raman modes in PZT ($x = 0.48$) studied through Eq. (2.3). Those calculated values of the Raman shifts were then fitted to the observed[20] data to get the coefficients a_0, a_1 and a_2 of the corrected function $A(P)$ (Eq. (2.4)) as given in Table 3 in the pressure intervals indicated. The calculated and observed[20] values of the Raman shifts of the Raman modes in PZT ($x = 0.48$) were given in Fig. 3.

As an extension of this work, the isothermal compressibility κ_T of the PZT ($x = 0.48$) ceramic was calculated by using its definition given by

$$\kappa_T = -\frac{1}{V}\left(\frac{\partial V}{\partial P}\right)_T, \tag{2.7}$$

Table 1. Values of the fitting parameters of Eq. (2.5) for the Raman modes in the PZT ($x = 0.48$) ceramic within the pressure interval indicated.

Cubic phase $T = 298$ K $P = 11.1$ GPa	Monoclinic phase $T = 298$ K $P = 0.1$ MPa	b_o (cm^{-1})	b_1 (cm^{-1}/GPa)	b_2 (cm^{-1}/GPa^2)	Pressure interval (GPa)
373 cm^{-1} (P_7F_{2u})	—	—	—	—	$0 < P < 4.5$
		352.758	2.583	−0.048	$5 < P < 17.8$
330 cm^{-1} (P_8)	328 cm^{-1}	329.799	−7.323	1.425	$0 < P < 4.5$
		315.564	1.100	0.039	$5 < P < 17.8$
243 cm^{-1} (P_9F_{2u})	275 cm^{-1}	275.103	2.399	−0.727	$0 < P < 4.5$
		264.111	−4.035	0.166	$5 < P < 17.8$
	252 cm^{-1}	252.187	−2.936	0.050	$0 < P < 4.5$
		264.111	−4.035	0.166	$5 < P < 17.8$
	224 cm^{-1}	222.611	−0.111	−0.518	$0 < P < 4.5$
		264.111	−4.035	0.166	$5 < P < 17.8$
199 cm^{-1} (P_9F_{1g})	204 cm^{-1}	205.741	−3.367	0.090	$0 < P < 4.5$
		223.146	−7.409	0.491	$5 < P < 11.1$
86 cm^{-1} ($P_{11}F_{2g}$)	143 cm^{-1}	144.723	−1.633	0.582	$0 < P < 4.5$
		49.123	4.309	−0.074	$7.8 < P < 17.8$
	126 cm^{-1}	126.822	−0.220	0.229	$0 < P < 4.5$
		49.123	4.309	−0.074	$7.8 < P < 17.8$
	112 cm^{-1}	110.447	7.018	−1.010	$0 < P < 4.5$
		49.123	−0.220	0.229	$7.8 < P < 17.8$

Table 2. Values of the fitting parameters of Eqs. (2.6) and (2.10) for the PZT ($x = 0.48$) ceramic within the pressure interval indicated.

Ceramic	V_0 (Å^3)	c_0 (Å^3)	c_1 (Å^3/GPa)	c_2(Å^3/GPa^2)	d_0(GPa)	d_1(GPa/K)	Pressure interval (GPA)
PZT ($x = 0.48$)	63.08	63.027	−1.047	0.100	—	—	$0 < P < 4.3$
		61.410	−0.303	0.003	—	—	$6.4 < P < 31.7$
		—	—	—	15.011	−0.023	$0 < P < 1$
		—	—	—	9.800	−0.016	$5 < P < 9$

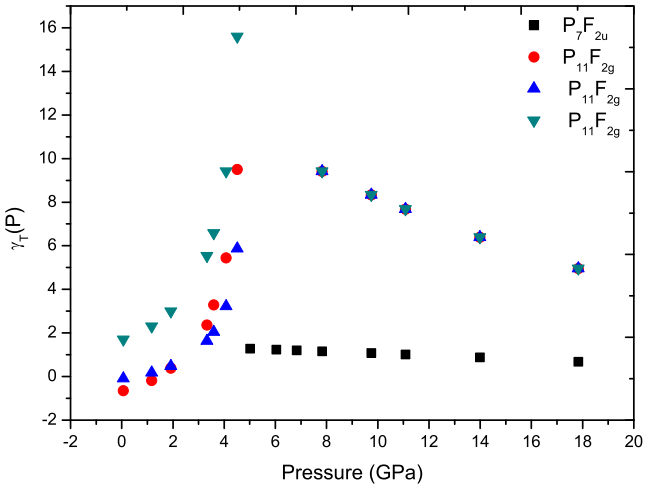

Fig. 1. Isothemal mode Grüneisen parameter $\gamma_T(P)$ calculated as a function of pressure for the Raman modes of P_7F_{2u} and triply degenerate $P_{11}F_{2g}$ close to the monoclinic-cubic transition ($P_C = 5$ GPa) in PZT ($x = 0.48$).

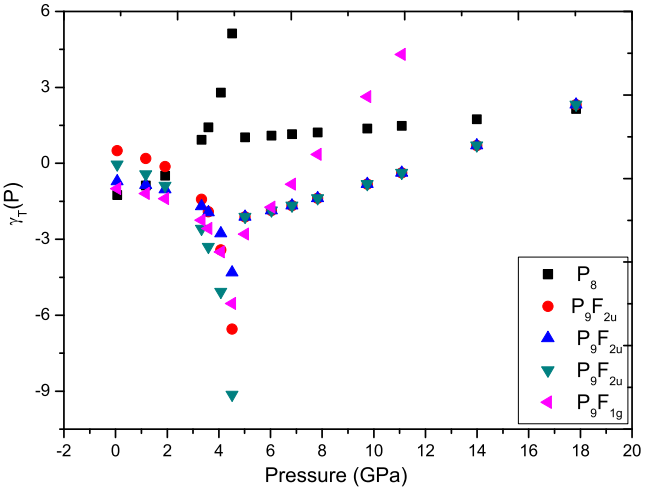

Fig. 2. Isothemal mode Grüneisen parameter $\gamma_T(P)$ calculated as a function of pressure for the Raman modes of P_8, triply degenerate P_9F_{2u} and P_9F_{1g} close to the monoclinic-cubic transition ($P_C = 5$ GPa) in PZT ($x = 0.48$).

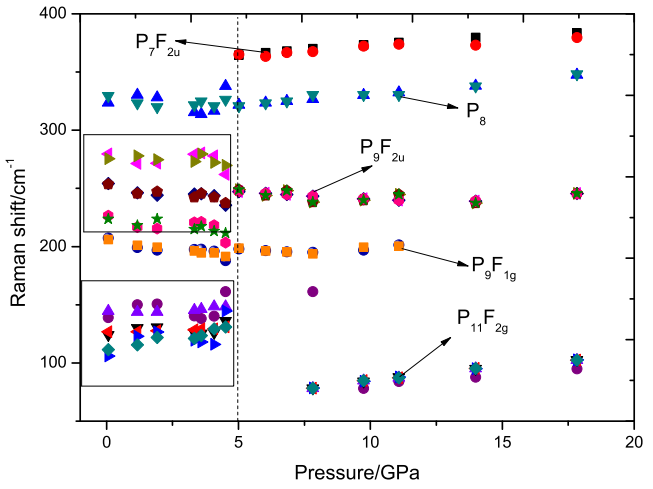

Fig. 3. Pressure dependence Raman shifts from the observed[38] volume data through the isothermal mode Grüneisen parameter $\gamma_T(P)$ for the Raman modes indicated in PZT ($x = 0.48$) according to Eq. (2.2). Observed[20] Raman shift data of those modes are also shown. The rectangles emphasize the triply degeneration of the $P_{11}F_{2g}$ and P_9F_{2u} Raman modes in the monoclinic phase of PZT ($x = 0.48$). The dashed line represents the transition pressure of $P_{Cn} = 5$ GPa.

inserting Eq. (2.6) in Eq. (2.7), one gets

$$\kappa_T = -\frac{2c_2P + c_1}{c_2P^2 + c_1P + c_0}, \tag{2.8}$$

so, the pressure dependence of κ_T (Eq. (2.8)) was calculated by using the fitting parameters of Eq. (2.6) (Table 2). Also, the thermal expansion α_P of the PZT ($x = 0.48$) ceramic was calculated by using the thermodynamic equation given as

$$\alpha_P = \kappa_T \frac{dP}{dT}, \tag{2.9}$$

for this calculation of α_P, the observed[20] P-T phase diagram of this ceramic was analyzed according to

$$P = d_0 + d_1T, \tag{2.10}$$

where d_0 and d_1 were constants with appropriate units, as given in Table 2 in the pressure intervals indicated. Finally, the specific heat $C_P - C_V$ of PZT ($x = 0.48$) ceramic can be evaluated using the thermodynamic relation given as

$$C_P - C_V = TV\left(\frac{dP}{dT}\right)\alpha_{p.} \tag{2.11}$$

Inserting the temperature T from Eq. (2.10) and the volume V from Eq. (2.6) into Eq. (2.11), the pressure dependence of the specific heat $C_P - C_V$ was calculated for PZT ($x = 0.48$) ceramic. The calculated values of the thermodynamic quantities isothermal compressibility κ_T, thermal expansion α_p and the specific heat $C_P - C_V$ of PZT ($x = 0.48$) ceramic studied here were given in Fig. 4 as a function of pressure.

3. Discussion

X-ray diffraction studies for pressure dependence of PZT ($x = 0.48$) ceramic at low temperatures of 44, 154 and 298 K by Rouquetta *et al.*[20,39] reported strong Raman spectra for the cubic paraelectric (P_C) phase that is contradictory with the

Table 3. Values of the fitting parameters of Eq. (2.4) for the Raman modes in the PZT ($x = 0.48$) ceramic within the pressure interval indicated.

Cubic phase $T = 298$ K $P = 11.1$ GPa	Monoclinic phase $T = 298$ K $P = 0.1$ MPa	a_o (cm^{-1})	a_1 (cm^{-1}/GPa)	a_2 (cm^{-1}/GPa^2)	Pressure interval (GPa)
373 cm^{-1} (P_7F_{2u})	—	—	—	—	$0 < P < 4.5$
		0.553	−0.149	0.046	$5 < P < 17.8$
330 cm^{-1} (P_8)	328 cm^{-1}	−6.960	19.689	−7.674	$0 < P < 4.5$
		−17.031	0.760	−0.112	$5 < P < 17.8$
243 cm^{-1} (P_9F_{2u})	275 cm^{-1}	5.354	−15.315	5.828	$0 < P < 4.5$
		−22.607	3.551	−0.384	$5 < P < 17.8$
	252 cm^{-1}	2.736	−7.686	2.882	$0 < P < 4.5$
		1.276	2.919	−0.338	$5 < P < 17.8$
	224 cm^{-1}	4.683	−14.228	5.614	$0 < P < 4.5$
		32.102	2.103	−0.279	$5 < P < 17.8$
199 cm^{-1} (P_9F_{1g})	204 cm^{-1}	2.738	−7.583	2.849	$0 < P < 4.5$
		0.448	5.831	−0.964	$5 < P < 11.1$
86 cm^{-1} ($P_{11}F_{2g}$)	143 cm^{-1}	−6.947	18.988	−6.779	$0 < P < 4.5$
		−110.285	−3.557	0.212	$7.8 < P < 17.8$
	126 cm^{-1}	−3.325	8.994	−3.194	$0 < P < 4.5$
		−90.663	−2.585	0.177	$7.8 < P < 17.8$
	112 cm^{-1}	−8.002	21.481	−7.534	$0 < P < 4.5$
		−74.159	−1.775	0.147	$7.8 < P < 17.8$

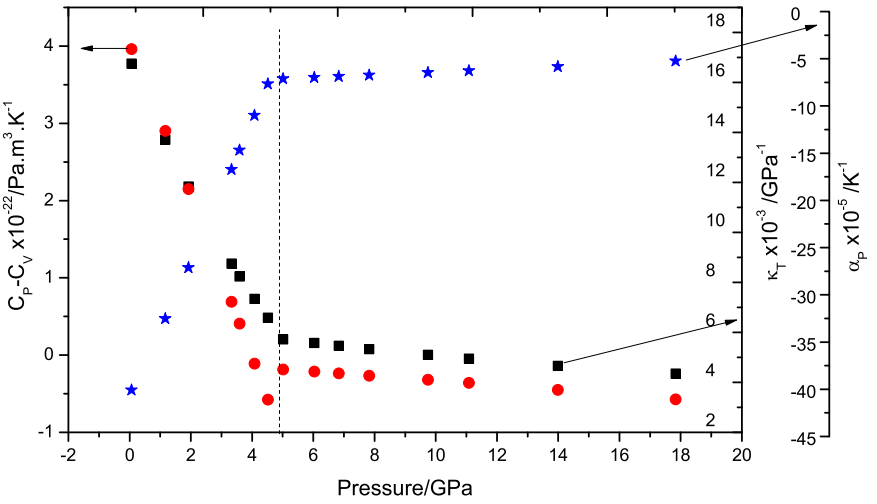

Fig. 4. Pressure dependence of the isothermal compressibility κ_T (Eq. (2.8)), thermal expansion α_P(Eq. (2.10)) and specific heat $C_P - C_V$ (Eq. (2.11)) from the observed[20] P-T data of PZT ($x = 0.48$) ceramic at room temperature of 300 K. The dashed line represents the transition pressure of $P_C = 5$ GPa.

expected first-order Raman spectra at high temperatures. They explained this contradiction via the presence of the static polar nanodomains in a tentatively new cubic form termed as "F_C" (rather than the cubic paraelectric phase P_C) that is characterized by static, symmetry-breaking disorder on a local level.[20] It is also indicated that a phase transition from monoclinic to disorder polar cubic ("F_C") take place at around 9, 7.5 and 5 GPa at constant low temperatures of 44, 154 and 298 K, respectively.[20] The observed bands in cubic $PbSc_{0.5}Nb_{0.5}O_3$ (PSN) ferroelectric relaxor[40] were very similar to that observed PZT ($x = 0.48$) ceramic[20] which leads to propose that vibrational modes in PSN are analogous to vibrational modes in PZT ($x = 0.48$) (Table 1 in Ref. 20). Five vibrational modes, namely P_7F_{2u}, P_8, P_9F_{2u}, P_9F_{1g} and $P_{11}F_{2g}$ in PZT ($x = 0.48$) at 298 K were observed.[20] Among them, P_7F_{2u} mode disappeared below 5 GPa (monoclinic phase) while P_9F_{2u} and $P_{11}F_{2g}$ modes decomposed into the three components at pressures $P < 5$ GPa and no decomposition was observed in monoclinic phase for P_8 and P_9F_{1g} modes. This decomposition of the $P_{11}F_{2g}$ Raman mode (disappearance of the Raman peaks in $110-145$ cm^{-1} region) at 5 GPa was characterized with the monoclinic-cubic ("F_C") transition in PZT ($x = 0.48$) ceramic.

The volume of the bulk PZT ($x = 0.48$) ceramic at 300 K was observed[33] to decrease as the pressure increases, particularly the discontinuity at around 4.2 GPa indicated a phase transition from tetragonal to paraelectric cubic (P_C) in this ceramic. This static compression data (V-P relation) for PZT ($X = 0.48$)[33] were analyzed according to Eq. (2.6) in the pressure intervals indicated as given in Table 2. These parameters of c_0, c_1 and c_2 (Table 2) were then used to calculate the isothermal Grüneisen parameter $\gamma_T(P)$ of these five observed vibrational modes[20] in cubic phase and also the decompositions of the P_9F_{2u} and $P_{11}F_{2g}$ modes in monoclinic phase of PZT ($x = 0.48$) at 298 K according to Eq. (2.2). The values of $\gamma_T(P)$ for P_7F_{2u} and triple degenerate $P_{11}F_{2g}$ Raman modes decreased while they increased for P_8, triply degenerated P_9F_{2u} and P_9F_{1g} as the pressure increased above the 5 GPa (cubic phase) up to 17 GPa as given in Fig. 1. Below 5 GPa (monoclinic phase), the $\gamma_T(P)$ values for the P_9F_{2u} and P_9F_{1g} Raman modes decreased (Fig. 2), on the contrary, they increased for P_8 and $P_{11}F_{2g}$ as the pressure increased (Figs. 1 and 2).

The wavenumbers shifts f of the Raman modes in PZT ($x = 0.48$) ceramic studied here were calculated according to the second term of Eq. (2.3) by using the values of the $\gamma_T(P)$ (Eq. (2.2)) close to the monoclinic-cubic ("F_C") transition pressure of 5 GPa. A fitting procedure for the calculated values of f and the observed data[20] allowed extracting the quadratic correction function $A(P)$ (Eq. (2.4)) with its coefficients in the pressure interval indicated as given in Table 3. No softening of the Raman wavenumber was calculated as also observed experimentally.[20] Figure 3 shows the harmony between the calculated (Eq. (2.3)) and the observed[20] pressure-dependent Raman wavenumber shifts of the modes are indicated in PZT ($x = 0.48$) ceramic. Investigation on the nanocrystalline PZT ceramic with different particle sizes showed the shifting in transition pressures.[21] It is indicated that the transition pressures decreases as the particle size increases. Calculation of the pressure-dependent Raman wavenumber shifts and the isothermal Grüneisen parameter $\gamma_T(P)$ from the bulk volume−pressure relation as performed in this study can also be done for the nanocrystalline PZT ceramics from the pressure-dependence of the unit cell volume of nanoparticles when they are available in the literature.

The isothermal compressibility κ_T of PZT ($x = 0.48$) ceramic was predicted through Eq. (2.8) as given in Fig. 4. κ_T decreases gradually at rates of -3.2×10^{-3} GPa^{-2} and -3.2×10^{-3} GPa^{-2} below and above the monoclinic-cubic

("F_C") transition pressure of 5 GPa, respectively. Additionally, the thermal expansion α_P and the specific heat $C_P - C_V$ of this ceramic were predicted according to Eqs. (2.10) and (2.11), respectively as given in Fig. 4. Those calculations of α_P and $C_P - C_V$ were performed by using the values of -2.3×10^{-3} GPa/K (monoclinic phase) and -1.6×10^{-2} GPa/K (cubic phase) for dP/dT extracted from the observed[20] P-T phase diagram of PZT ($x = 0.48$) crystal. The results were as follows, $C_P - C_V$ decreases gradually at rates of $-7.4 \times 10^{-2}\,\mathrm{GPa}^{-1}$ below 5 GPa (monoclinic phase) and -3.5×10^{-3} above 5 GPa (cubic phase) while α_P increases gradually at rates of $7.3 \times 10^{-5}\,\mathrm{K}^{-1}\mathrm{GPa}^{-1}$ and $1.5 \times 10^{-6}\,\mathrm{K}^{-1}\mathrm{GPa}^{-1}$ in the monoclinic and cubic phases, respectively.

4. Conclusions

Bulk volume data of PZT ($x = 0.48$) ceramic obtained at room temperature (300 K) as a function of pressure was used from the literature to calculate the isothermal Grüneisen parameter of the Raman modes in this ceramic. That simple definition of the microscopic mode Grüneisen parameter makes it possible to determine the spectroscopic quantity such as wavenumber shifts of perovskite crystals as done for PZT ($x = 0.48$) ceramic in this study. The calculated values of the wavenumber shift for the Raman modes in PZT ($x = 0.48$) ceramic by means of the isothermal Grüneisen parameter agree well with the observed data. Also, the thermodynamic quantities such as specific heat, isothermal compressibility and thermal expansion of PZT ($x = 0.48$) ceramic were also predicted and discussed as a function of pressure. Those calculated thermodynamic quantities for PZT ($x = 0.48$) can be compared with the experimental data when they are available in the literature which may lead extracting the Grüneisen parameter of the Raman modes in PZT ($x = 0.48$) ceramic from its macroscopic definition.

Acknowledgment

I would like to thank Prof. H. Yurtseven for his valuable and useful comments on this study.

References

[1]S. K. Mishra, A. P. Singh and D. Pandey, Effect of phase coexistence at morphotropic phase boundary on the properties of $Pb(Zr_xTi_{1-x})O_3$ ceramics, *Appl. Phys. Lett.* **69**, 1707 (1996).

[2]S. K. Mishra, A. P. Singh and D. Pandey, Thermodynamic nature of phase transitions in $Pb(Zr_xTi_{1-x})O_3$ ceramics near the morphotropic phase boundary. I. Structural studies, *Philos. Mag. B.* **76**, 213 (1997).

[3]S. K. Mishra and D. Pandey, Thermodynamic nature of phase transitions in $Pb(Zr_xTi_{1-x})O_3$ ceramics near the morphotropic phase boundary. II. Dielectric and piezoelectric studies, *Philos. Mag. B.* **76**, 227 (1997).

[4]B. Jaffe, W. R. Cook and H. Jaffe, *Piezoelectric Ceramics*, (Academic Press, London, 1971).

[5]G. Shirane *et al.*, Phase transitions in solid solutions of $PbZrO_3$ and $PbTiO_3$ (I) small concentrations of $PbTiO_3$, *J. Phys. Soc. Jpn.* **7**, 5 (1952).

[6]B. Noheda, D. E. Cox, G. Shirane, J. A. Gonzalo, L. E. Cross and S.-E. Park, A monoclinic ferroelectric phase in the $Pb(Zr_{1-x}Ti_x)O_3$ solid solution, *Appl. Phys. Lett.* **74**, 2059 (1999).

[7]B. Noheda, J. A. Gonzalo, L. E. Cross, R. Guo, S.-E. Park, D. E. Cox and G. Shirane, Tetragonal-to-monoclinic phase transition in a ferroelectric perovskite: The structure of $PbZr_{0.52}Ti_{0.48}O_3$, *Phys. Rev. B.* **61**, 8687 (2000).

[8]B. Noheda, D. E. Cox, G. Shirane, R. Guo, B. Jones and L. E. Cross, Stability of the monoclinic phase in the ferroelectric perovskite $Pb(Zr_{1-x}Ti_x)O_3$, *Phys. Rev. B.* **63**, 014103 (2001).

[9]R. R. Ragini, S. K. Mishra, D. Pandey, H. Lemmens and G. Van Tendeloo, Evidence for another low-temperature phase transition in tetragonal $Pb(Zr_{1-x}Ti_x)O_3$ ($x = 0.515$–0.520), *Phys. Rev. B.* **64**, 054101 (2001).

[10]R. R. Ragini, S. K. Mishra, D. Pandey and B. J. Kennedy, Antiferrodistortive phase transition in $Pb(Ti_{0.48}Zr_{0.52})O_3$: A powder neutron diffraction study, *Phys. Rev. B.* **65**, 060102 (2002).

[11]D. M. Hatch, H. T. Stokes, R. R. Ragini, S. K. Mishra, D. Pandey and B. J. Kennedy, Antiferrodistortive phase transition in $Pb(Ti_{0.48}Zr_{0.52})O_3$: Space group of the lowest temperature monoclinic phase, *Phys. Rev. B.* **65**, 212101 (2002).

[12]K. Kakewaga, O. Matsunaga, T. Kato and Y. Sasaki, Sluggish pansition between tetragonal and rhombohedral phases of Pb(Zr, Ti)O_3 prepared by application of electric field, *J. Am. Ceram. Soc.* **78**, 1071 (1995).

[13]J. F. Meng, R. S. Katiyar, G. T. Zou and X. H. Wang, Raman phonon modes and ferroelectric phase transitions in nanocrystalline lead zirconate titanate, *Phys. Stat. Sol. A.* **164**, 851 (1997).

[14]F. Jona and G. Shirane, *Ferroelectric Crystals* (Dover Publications, New York, 1993).

[15]E. B. Araújo, K. Yukimitu, J. C. S. Moraes, L. H. Z. Pelaio and J. A. Eiras, Monoclinic-tetragonal phase transition in $Pb(Zr_{1-x}Ti_x)O_3$ studied by infrared spectroscopy, *J. Phys. Condens. Matter.* **14**, 5195 (2002).

[16]C. A. Guarany, L. H. Z. Pelaio, E. B. Araújo, K. Yukimitu, J. C. S. Moraes and J. A. Eiras, Infrared studies of the monoclinic–tetragonal phase transition in Pb(Zr,Ti)O_3 ceramics, *J. Phys. Condens. Matter.* **15**, 4851 (2003).

[17]E. B. Araújo, C. A. Guaranu, K. Yukimutu, J. C. S. Moraes and J. A. Eiras, Structural phase transitions of $PbZr_{0.52}Ti_{0.48}O_3$ ceramic: An infrared spectroscopy study, *Ferroelectrics* **337**, 145 (2006).

[18]A. G. Souza Filho, K. C. V. Lima, A. P. Ayala, I. Guedes, P. T. C. Freire, J. Mendes Filho, E. B. Araújo and J. A. Eiras, Monoclinic phase of $PbZr_{0.52}Ti_{0.48}O_3$ ceramics: Raman and phenomenological thermodynamic studies, *Phys. Rev. B.* **61**, 14283 (2000).

[19]K. C. V. Lima, A. G. Ouza Filho, A. P. Ayala, J. Mendes Filho, P. T. C. Freire, F. E. A. Melo, E. B. Araújo and J. A. Eiras, Raman study of morphotropic phase boundary in $PbZr_{1-x}Ti_xO_3$ at low temperatures, *Phys. Rev. B.* **63**, 1841051 (2001).

[20]J. Rouquette, J. Haines, V. Bornand, M. Pintard, Ph. Papet, B. Bennet and F. A. Gorelli, P-T phase diagram of $PbZr_{0.52}Ti_{0.48}O_3$ (PZT), *Sol. Stat. Sci.* **5**, 451 (2003).

[21]Z. Yuan, J. Zhu, S. Zhang, X. Wang, L. Li and C. Jin, Raman spectroscopy studies of nanocrystalline lead zirconate titanate as functions of particle size and pressure, *Spectr. Lett.* **48**, 521 (2015).

[22]R. Guo, L. E. Cross, S. E. Park, B. Noheda, D. E. Cox and G. Shirane, Origin of the high piezoelectric response in $PbZr_{1-x}Ti_xO_3$, *Phys. Rev. Lett.* **84**, 5423 (2000).
[23]E. Buixaderas, V. Bovtun, M. Kempa, D. Nuzhnyy, M. Savinov, P. Vanek, I. Gregora and B. Malic, Lattice dynamics and domain wall oscillations of morphotropic $Pb(Zr,Ti)O_3$ ceramics, *Phys. Rev. B.* **94**, 054315 (2016).
[24]V. Y. Topolov and A. V. Turik, A new monoclinic phase and features of stress relief in $PbZr_{1-x}Ti_xO_3$ solid solutions, *J. Phys. Condens. Matter.* **13**, L771 (2001).
[25]W. R. Biessem, L. E. Cross and A. K. Goswami, Phenomenological theory of high permittivity in fine-grained barium titanate, *J. Am. Ceram. Soc*. **1**, 36 (1966).
[26]Q. M. Zhang, J. Zhao, K. Uchino and J. Zheng, Change of the weak-field properties of $Pb(ZrTi)O_3$ piezoceramics with compressive uniaxial stresses and its links to the effect of dopants on the stability of the polarizations in the materials, *J. Mater. Res.* **12**, 226 (1997).
[27]Q. M. Zhang and Z. Jianzhong, Electromechanical properties of lead zirconate titanate piezoceramics under the influence of mechanical stresses, *IEEE Trans. Ultrason. Ferroelectr. Freq. Control.* **46**, 1518 (1999).
[28]D. Damjanovic, Stress and frequency dependence of the direct piezoelectric effect in ferroelectric ceramics, *J. Appl. Phys.* **82**, 1788 (1997).
[29]D. Audigier, Cl. Richard, Cl. Deschamps, M. Troccaz and L. Eyraud, PZT uniaxial stress dependence: Experimental results, *Ferroelectrics* **154**, 219 (1994).
[30]M. Pisarski, Morphotropy region under high hydrostatic pressure in PZT-systems, *Ferroelectrics* **94**, 215 (1989).
[31]H. Yurtseven and A. Kiraci, Damping constant (linewidth) and the relaxation time of the brillouin LA mode for the ferroelectric-paraelectric transition in $PbZr_{1-x}Ti_xO_3$, *IEEE Trans. Ultrason. Ferroelectr. Freq. Control.* **63**, 1647 (2016).
[32]E. Buixaderas, I. Gregora, S. Kamba, J. Petzelt and M. Kosec, Raman spectroscopy and effective dielectric function in PLZT x/40/60, *J. Phys. Condens. Matter.* **20**, 345229 (2008).
[33]I. A. Kornev, L. Bellaiche, P. E. Janolin, B. Dkhil and E. Suard, Phase diagram of $Pb(Zr,Ti)O_3$: Solid solutions from first principles, *Phys. Rev. Lett.* **97**, 157601 (2006).
[34]J. Frantti, S. Ivanov, J. Lappalainen, S. Eriksson, V. Lantto, S. Nishio, K. Kakihana and H. Rodolf, Local and average structure of lead titanate based ceramics, *Ferroelectrics* **266**, 73 (2002).
[35]T. H. K. Barron, Grüneisen parameters for the equation of state of solids, *Ann. Phys.* **1**, 77 (1957).
[36]J. P. Poirier, *Introduction to the Physics of the Earth's Interior* (Virtual Publishing, Cambridge, 1991).
[37]A. Kiraci and H. Yurtseven, Pressure dependent raman modes near the cubic-tetragonal transition in strontium titanate, *J. Am. Ceram. Soc.* **101**, 1344 (2018).
[38]K. H. Cho, C. E. Seo, Y. S. Choi, Y. H. Ko and K. J. Kim, Effect of pressure on electric generation of PZT(30/70) and PZT(52/48) ceramics near phase transition pressure, *J. Eur. Ceram. Soc.* **32**, 457 (2012).
[39]J. Rouquette, J. Haines, V. Bornand, M. Pintard, Ph. Papet, R. Astier, J. M. Léger and F. Gorelli, Transition to a cubic phase with symmetry-breaking disorder in $PbZr_{0.52}Ti_{0.48}O_3$ at high pressure, *Phys. Rev. B.* **65**, 214102 (2002).
[40]I. G. Siny and C. Boulesteix, On the paraelectric phase structure of $AB'_xB''_{1-x}O_3$-type compounds, *Ferroelectrics* **96**, 119 (1989).